

# Single-Channel Beta–Gamma Coincidence Detection of Radioactive Xenon Using Digital Pulse Shape Analysis of Phoswich Detector Signals

Wolfgang Hennig, *Member, IEEE*, Hui Tan, William K. Warburton, *Member, IEEE*, and Justin I. McIntyre

**Abstract**—Monitoring radioactive xenon in the atmosphere is one of several methods used to detect nuclear weapons testing. To increase sensitivity, monitoring stations use a complex system of separate beta and gamma detectors to detect beta–gamma coincidences from the Xe isotopes of interest, which is effective but requires such careful gain matching and calibration that it is difficult to operate in the field. To simplify the system, a phoswich detector has been designed, consisting of optically coupled plastic and CsI scintillators to absorb beta particles and gamma rays, respectively. Digital pulse shape analysis (PSA) of the detector signal is used to determine if radiation interacted in either or both parts of the detector and to measure the energy deposited in each part, thus using only a single channel of readout electronics to detect beta–gamma coincidences and to measure both energies. Experiments with a prototype detector show that the technique can clearly separate event types, does not degrade the energy resolution, and has an error rate for detecting coincidences of less than 0.1%. Monte Carlo simulations of radiation transport and light collection in the proposed detector were performed to obtain optimum values for its design parameters and an estimate of the coincidence detection efficiency (82%–92%) and the background rejection rate (better than 99%).

**Index Terms**—Beta–gamma coincidence detection, digital pulse shape analysis, phoswich detector, radioxenon monitoring.

## I. INTRODUCTION

MONITORING radioactive xenon in the atmosphere is one of several methods currently employed to detect nuclear weapons testing as part of the Comprehensive Nuclear-Test-Ban Treaty. A monitoring station, such as the Automated Radioxenon Sampler and Analyzer (ARSA) developed at Pacific Northwest National Laboratory (PNNL) [1], extracts Xe from large volumes of air and then measures its radioactivity in an extremely low background counter. Since the four Xe isotopes of interest, listed in Table I, all emit one or more beta particles or conversion electrons simultaneously with one or more gamma rays or X-rays, beta–gamma coincidence can be used to suppress the counter’s natural background rate. Analysis of the beta and gamma energy spectra is then used to identify which isotopes are present in a sample.

Manuscript received November 15, 2005; revised January 18, 2006. This work was supported by the U.S. Department of Energy under Award No. DE-FG02-04ER84121.

W. Hennig, H. Tan, and W.K. Warburton are with XIA LLC, Newark, CA 94560 USA (e-mail: whennig@xia.com).

J. I. McIntyre is with Pacific Northwest National Laboratory, Richland, WA 99352 USA.

Digital Object Identifier 10.1109/TNS.2006.870447

TABLE I  
XE ISOTOPES USED FOR NUCLEAR MONITORING AND THEIR CHARACTERISTIC RADIATIONS (keV)

Isotope	$^{131m}\text{Xe}$	$^{133m}\text{Xe}$	$^{133g}\text{Xe}$	$^{135g}\text{Xe}$
X-rays	30	30	31	31
gamma rays	163.9	233.2	81.0	249.8
beta particles	-	-	346 (max.)	905 (max.)
conversion electrons	129	199	45	214

Commonly used time-based coincidence detection using separate detectors for beta and gamma radiation requires several channels of photomultiplier tubes (PMTs) and readout electronics: in case of the ARSA system, a total number of 12 for four sample cells. This leads to complex and bulky detector systems that require careful gain matching and calibration. In one approach to simplify the system [2], researchers at PNNL explored the use of a phoswich detector made from two scintillator materials with slow (940 ns) and fast (250 ns) decay times to detect beta and gamma radiation, respectively. The phoswich detector was read out by a single PMT with an integrating preamplifier, thus generating slow- or fast-rising pulses depending on which scintillator was hit. Rise time analysis of acquired pulse waveforms was used to classify interactions as occurring in either or both parts of the detector.

This method worked well to distinguish radiation interacting in any single part of the detector, but radiation interacting in both parts—corresponding to the beta–gamma coincidences required for radioxenon monitoring—were not easily identified using this algorithm, instrumentation, and particular choice of scintillators, and it was deemed almost impossible to measure the beta and gamma energies separately.

In this paper, we describe an improved phoswich detector and pulse shape analysis (PSA) method that can both detect beta–gamma coincidences and measure the energies accurately.

## II. MEASUREMENTS WITH PLANAR PHOSWICH DETECTOR

A prototype of the improved phoswich detector consists of a 1-mm-thick, 25.4-mm-diameter disk of the fast plastic scintillator BC-404, optically coupled to a 25.4-mm-long cylinder of the slow scintillator CsI(Tl), as shown in the inset of Fig. 1. Beta particles and conversion electrons are absorbed in the BC-404, while longer range gamma rays and X-rays are mainly absorbed in the CsI. The phoswich detector is read out by a single PMT

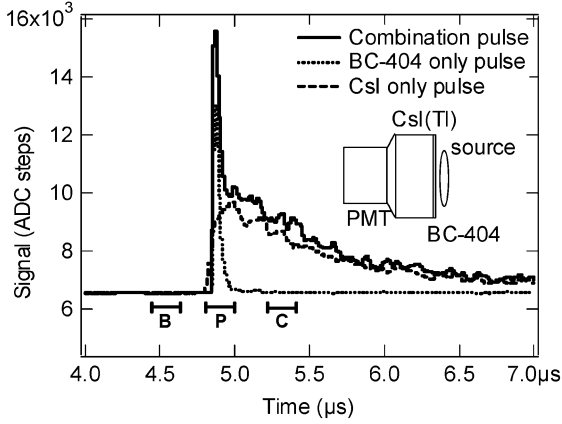


Fig. 1. Pulse shapes from the planar prototype phoswich detector illustrated in the inset, using a  $^{60}\text{Co}$  reference source.

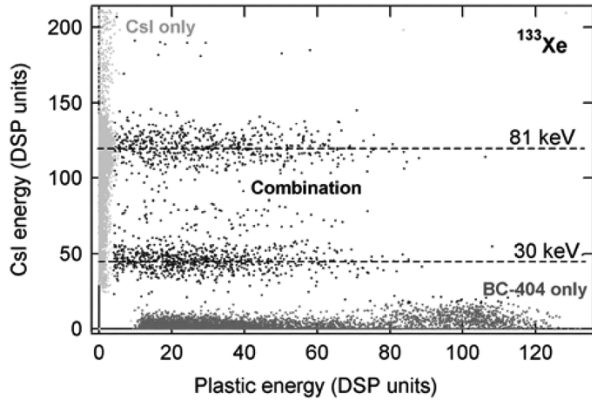


Fig. 2. Energy scatter plot for data acquired with a  $^{133}\text{Xe}$  gas standard, shaded by event type. CsI only events fall on the vertical axis, BC-404 only events fall on the horizontal axis, and the majority of coincidence events form horizontal bands at characteristic X-ray or gamma ray energies (fixed photon energy deposited in the CsI and varying beta energy deposited in the BC-404).

directly connected to an XIA DGF Pixie-4, a high-speed digital pulse processor [3]. The scintillator time constants are sufficiently different to clearly separate three pulse types as shown in Fig. 1: a) slow-rising and slow-falling pulses corresponding to interactions only in the CsI, b) very fast pulses with high amplitude corresponding to interactions only in the BC-404, and c) combinations of the previous cases corresponding to coincident interactions in both scintillators.

For initial testing and the development of the PSA algorithms, the prototype detector was used with solid reference sources such as  $^{137}\text{Cs}$ ,  $^{241}\text{Am}$ , and  $^{60}\text{Co}$ . In later measurements, the prototype detector was used with small amounts of  $^{133}\text{Xe}$  and  $^{220}\text{Rn}$  gas standards enclosed in plastic bags and placed in front of the detector.

A digital trapezoidal filter with a rise time of  $\sim 7 \mu\text{s}$ , implemented in field programmable gate arrays of the Pixie-4, provided a measure of the overall pulse energy  $E$ . In addition, waveforms were acquired for each pulse and the Pixie-4's on-board digital signal processor (DSP) calculated the sum  $B$  in the baseline region, the sum  $P$  in the plastic pulse region, and the sum  $C$  in the region of the decaying CsI pulse as indicated in Fig. 1, as well as the signal rise time. These quantities were used in the offline PSA as described below.

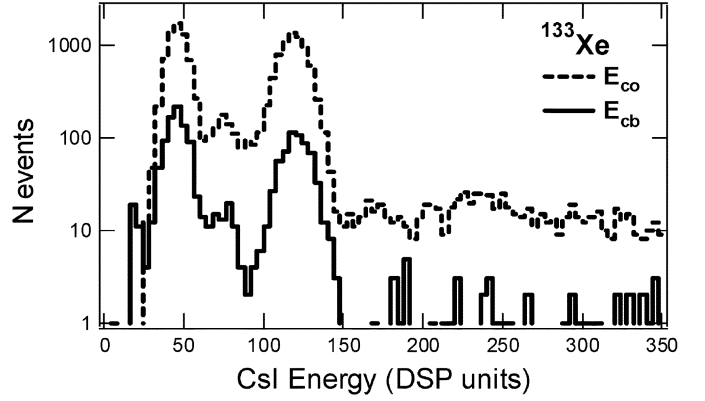


Fig. 3. Histogram of energy deposited in CsI for CsI only events ( $E_{co}$ ) and for combination events ( $E_{cb}$ ). The energy resolution at the 81 keV peak at bin  $\sim 120$  is 16.9% for  $E_{co}$  and 17.1% for  $E_{cb}$ .

### III. RESULTS AND DISCUSSION

#### A. PSA Development to Detect Coincidences

For radioxenon monitoring applications, the system has to be able to detect beta–gamma coincidences and to measure both beta and gamma energy with good precision. Using the data acquired with the prototype detector, we therefore developed PSA algorithms to separate the combination events from the other event types and to find the energy deposited in each part of the phoswich detector. Since the detector, electronics, digital filters, and DSP sums together form a linear system, we assume that the energy  $E$  and the sums  $B$ ,  $P$ , and  $C$  are linear combinations of CsI and BC-404 contributions (e.g.,  $E = E_p + E_c$ ), where the index  $p$  refers to contributions from the plastic scintillator BC-404 and the index  $c$  to contributions from the CsI.

In the analysis, we first select all events with  $C \sim B$  (i.e., BC-404 only events in which all contributions from the CsI are zero) and determine from them the calibration factor  $a = E_p/(P_p - B_p)$ . From all events with  $C > B$  and  $(P - B)$  below a threshold  $T$  (i.e., CsI only events where all contributions from BC-404 are zero), we determine the calibration factor  $b = E_c/(P_c - B_c)$ . The calibration factors are then used to determine for each event the individual energies  $E_c$  and  $E_p$  from the measured quantities  $E$ ,  $P$ , and  $B$ :

$$\begin{aligned} E_c &= (E - a * (P - B)) / (1 - a/b) \\ E_p &= E - E_c. \end{aligned} \quad (1)$$

The acquired events can then be displayed in two-dimensional (2-D) energy scatter plots as shown in Fig. 2 for data from a  $^{133}\text{Xe}$  gas standard. The event types fall into three clearly separated groups, and by defining thresholds in both CsI and BC-404 energy, events from each group can be binned in separate energy histograms. For events with small values of  $E_p$ , the signal rise time can be additionally used to better separate fast rising BC-404 only or combination events from slow rising CsI only events.

Fig. 3 shows the histograms of the energy deposited in CsI for CsI only events ( $E_{co}$ ) and for combination events ( $E_{cb}$ ) for the same  $^{133}\text{Xe}$  source as in Fig. 2; as expected, BC-404 only events deposit zero energy in the CsI within the error of the measurement, and their CsI energy histogram is not displayed.

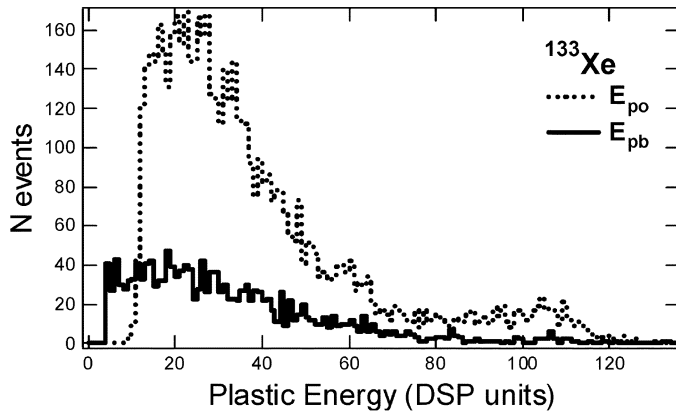


Fig. 4. Histogram of energy deposited in BC-404 for BC-404 only events ( $E_{po}$ ) and for combination events ( $E_{pb}$ ).

TABLE II  
FRACTIONS OF EVENT TYPES FROM  $^{241}\text{Am}$

Events classified as	No alpha shield		With alpha shield	
CsI only	214284	63.1%	320947	94.5%
BC-404 only	100555	29.6%	630	0.2%
Combination	11706	3.4%	379	0.1%
Other	12955	3.8%	17544	5.2%
Total	339500		339500	

Fig. 4 shows the histograms of the energy deposited in BC-404 for BC-404 only events ( $E_{po}$ ) and for combination events  $E_{pb}$  for the same data acquisition.

The resolution for energy deposited in the CsI is comparable for CsI only and combination events, e.g., 5.2% and 5.4% for the 1.3 MeV peak of  $^{60}\text{Co}$ , respectively. This resolution is about equal to values achieved with standard CsI detectors and demonstrates that the PSA algorithms do not degrade the measured energy. Note that in Fig. 3, the resolution for the 81 keV peak is about 17%, better than the 25% reported for the existing ARSA detector, and even good enough to resolve the iodine escape peak at about bin number 75.

The prototype detector was illuminated with an  $^{241}\text{Am}$  source to test the reliability of the PSA algorithms.  $^{241}\text{Am}$  emits alpha particles and gamma rays in coincidence, and the gamma ray energies of 59.5 keV and 26.5 keV are similar to characteristic energies from radioxenon (30 keV X-rays; 81 keV and higher energy gamma rays). As the alpha particles will be absorbed in the BC-404 and the gamma rays will mainly be absorbed in the CsI, we expect to find combination events due to alpha–gamma coincidences similar to the beta–gamma coincidences observed with  $^{133}\text{Xe}$ . Table II shows that about 3.4% of all detected events are such combination events.

On the other hand, when a thin sheet of Al is inserted between source and detector to shield the detector from alpha particles, the coincidences are suppressed. Any remaining combination events found by the PSA must be due to either Compton scattering of gamma rays between BC-404 and CsI, random coincidences, or classification errors by the PSA. For a worst case estimate of the PSA error rate, we consider *all* observed combination events to be errors of the PSA. As shown in Table II, the fraction of combination events with an alpha shield is 0.1%,

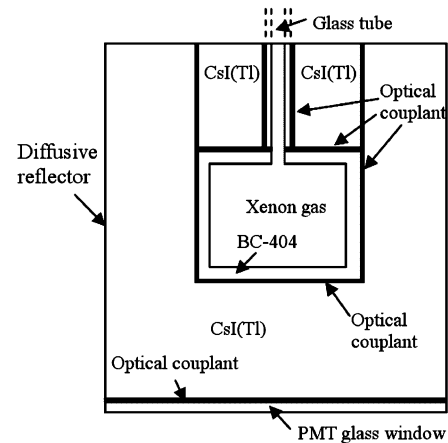


Fig. 5. Geometry of the proposed phoswich well detector. The outer dimensions of the CsI cylinder are 76.2 mm long by 76.2 mm diameter; the BC-404 cell is 25.4 mm long by 25.4 mm diameter

and thus the rate of the PSA to wrongly classify a CsI only or BC-404 only event as a coincidence is at most 0.1% at the energies studied.

Of the detected events listed in Table II, 3%–5% cannot be classified clearly as any of the three event types by the PSA and are categorized as “other.” These events may serve as a very crude estimate of the overall efficiency of the algorithm. While most of the “other” events are simply near-noise events with both  $E_c$  and  $E_p$  close to zero, we can assume in a worst case estimate that all of them are valid events, but that the PSA failed to determine the event type. This means that the efficiency of the PSA to correctly classify events is at least 95% to 97%.

### B. Design of Phoswich Well Detector

While the prototype detector was sufficient to develop the PSA algorithms for detecting coincidences and measuring individual energies with good precision in a single channel of electronics, it has very low coincidence detection efficiency since at least half of the beta radiation and the gamma radiation will be emitted away from the detector. Using Monte Carlo simulations of light collection and radiation transport, we therefore studied a phoswich well detector design in which a BC-404 cell holding the radioxenon is enclosed in a 76.2 mm cylinder of CsI (see Fig. 5).

1) *Light Collection Simulations:* The unusual geometry of the phoswich well detector will affect its uniformity of light collection. We therefore carried out Monte Carlo simulations of the light collection for the proposed well detector geometry, the planar prototype detector, and other geometries using the Monte Carlo code DETECT2000 [4]. Fig. 6 shows the distribution of light collection efficiency in the well detector with a reflectivity of 0.95 or 0.99 for the diffusive reflector on the outer surface of CsI. We found that placing a structure inside the CsI crystal somewhat degrades the uniformity of the light collection efficiency, especially if the coating on the outside of the CsI crystal has a low reflection coefficient. From the volume-weighted probability distribution of the light collection efficiency, we estimate that the energy resolution of mono-energetic gamma rays, due only to the nonuniformity of the collection efficiency in the crystal, increases from 2.4% without a

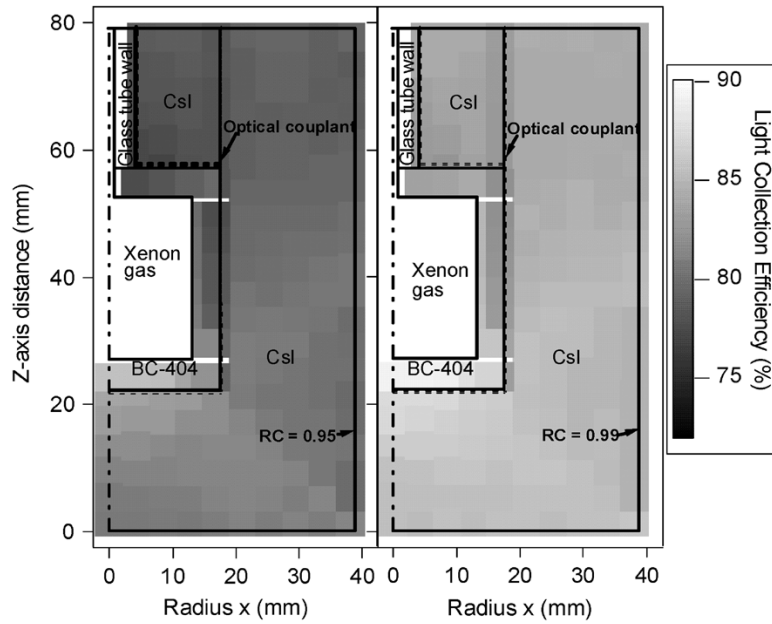


Fig. 6. Light collection efficiency in the proposed phoswich well detector. A higher reflectivity of the outer surface results in a higher efficiency and a more uniform distribution throughout the detector. By symmetry, only half of the detector was simulated.

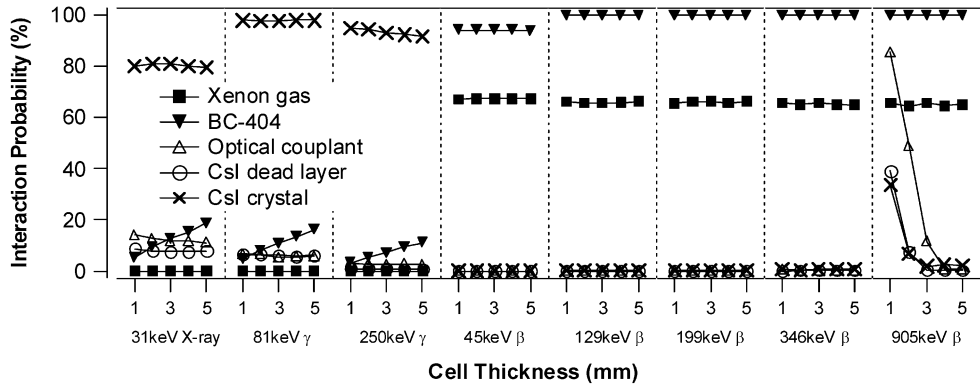


Fig. 7. Interaction probability of major radioxenon decay energies in each component of the phoswich well detector for radiation emitted from the center of the BC-404 cell. Radiation may interact with more than one component, so the sum of probabilities in a column may exceed 100%.

cell to 2.9% with a spherical cell and 3.8% with a cylindrical cell (for the conservative estimate of the reflectivity, i.e., 0.95). However, compared to a typical measured resolution of  $\sim 7\%$  at 662 keV (resulting from photostatistics, crystal nonuniformities and energy nonlinearities), the effects of the embedded cell, added in quadrature, are small. We thus anticipate that the phoswich detector energy resolution will not be significantly worsened at the lower energies from the Xe isotopes due to effects of light collection, provided that the reflectivity is kept high and the cell is not unreasonably shaped.

2) *Radiation Transport Simulations:* Monte Carlo simulations of the radiation transport in the phoswich detector were performed to determine optimum values of design parameters and to estimate the coincidence detection efficiency. Using the Monte Carlo code PENELOPE, several characteristic energies of gamma rays, X-rays, beta particles and conversion electrons from the four Xe isotopes of interest were simulated for the well detector and also for the prototype detector, in order to compare the simulation to the experiments. In the simulation, beta particles were assumed to all have the end-point energy, not a con-

tinuous energy distribution and thus only five discrete energy values were simulated for beta particles and conversion electrons. This approximation was sufficient for our primary purpose of studying the maximum range of the particles and determining the detector elements they will interact with.

The simulations showed that most beta particles or conversion electrons will be absorbed in the BC-404 and most X-rays or gamma rays will be absorbed in the CsI, as intended (see Fig. 7). A small fraction of high-energy gamma rays will escape from the detector, and a small fraction of low energy beta particles will be absorbed in the xenon gas, i.e., they will not be detected. The thickness of the BC-404 cell has to be adjusted to compromise between preventing betas from reaching the CsI (thicker wall) and reducing the chance of photons interacting with the plastic (thin wall). A wall thickness of 2 to 3 mm is a good compromise: the fraction of betas with full 905 keV reaching the CsI is 7% (2%) for a 2 mm (3 mm) wall, but 33% for a 1 mm wall; the fraction of photons interacting with the plastic is 5%–9% (7%–12%) for a 2 mm (3 mm) wall, but 3%–6% for a 1 mm wall.

TABLE III  
PROBABILITIES (IN %) OF SIMULTANEOUS INTERACTIONS OF A  
CHARACTERISTIC GAMMA RAY AND BETA PARTICLE FROM  $^{133g}\text{Xe}$

Interactions of		Beta (346keV)			
		none	BC-404 only	CsI only	both
Gamma (81keV)	none	0.0	1.5	0.0	0.0
	BC-404 only	0.0	0.3	0.0	0.0
	CsI only	0.0	<b>92.6</b>	0.0	0.5
	both	0.0	5.1	0.0	0.0

TABLE IV  
PROBABILITIES (IN %) OF SIMULATED EXTERNAL GAMMA RAYS TO INTERACT  
WITH THE PHOSWICH WELL DETECTOR

Gamma Energy (MeV)	none	BC-404 only	CsI only	both	both, < 250keV deposited in CsI
0.583	8.66	0.22	88.95	2.17	0.86
1.461	24.20	0.49	73.05	2.26	0.82
2.614	30.18	0.48	66.87	2.47	0.68
5	32.35	0.14	64.33	3.18	0.22
10	29.08	0.05	65.55	5.32	0.07
20	23.22	0.01	66.70	10.07	0.01

The interaction probabilities of the characteristic energies were then used to obtain an estimate of the coincidence detection efficiency. For example, 81 keV gamma rays and 346 keV beta particles may be taken to represent the coincidence radiation from  $^{133g}\text{Xe}$ . Each has a certain probability to interact i) not at all, ii) with BC-404 only, iii) with CsI only, or iv) with both BC-404 and CsI. The products of the probabilities for the altogether 16 combinations are shown in Table III. Events where betas interact only with the BC-404 and gammas interact only with the CsI are coincidence events with good energy measurement, shown in bold in Table III. For  $^{133g}\text{Xe}$ , the estimated coincidence detection efficiency of the well detector is thus 92.6%, for the other three xenon isotopes of interest it is about 82%.

Though the well detector will be shielded during operation, some background radiation from the detector enclosure, the environment or cosmic sources will still interact with the detector. To estimate the rejection ratio of the well detector to such background events, we also simulated gamma rays of various energies coming from a single external location and directed toward the center of the detector (Table IV). Most events interact with the CsI only and will be rejected by the PSA. Between 2% to 10% of simulated events interact with both scintillators, but only 0.9% to 0.01% of the events will be coincident *and* deposit less

than 250 keV in the CsI, the maximum gamma ray energy from the xenon decay chain.

In practice, the background radiation will have a multitude of origins and most of it will not be directed toward the center of the detector, i.e., only interacting with the CsI and rejected by the PSA (unless scattered into the BC-404). As a crude estimate, we assume that the simulation represents only 1/27th of the total background radiation (the volume fraction of the BC-404 cell in the detector) and that the rest will not interact with the BC-404 cell at all. This means the numbers in the last column of Table IV have to be divided by 27 and that overall the background rejection ratio for the phoswich well detector is greater than 99.9% in the energy range of interest.

#### IV. CONCLUSION

In summary, we developed an algorithm to detect beta-gamma coincidences in the signals from a BC-404/CsI(Tl) phoswich detector, using a single channel of readout electronics. The algorithm achieves clear separation of BC-404 only, CsI only, and combination events, accurate measurement of the individual energies deposited in BC-404 and CsI, and has an error rate for detecting coincidences of less than 0.1%. Less than 3% to 5% of detected events cannot be classified as any of the three event types.

Monte Carlo simulations of radiation transport and light collection were performed to optimize design parameters for a replacement detector module for the ARSA system, obtaining an estimated coincidence detection efficiency of 82% to 92% and a background rejection ratio better than 99%. The new phoswich/pulse shape analysis method is thus suitable to simplify the existing ARSA detector system to the level of a single detector per sample chamber while maintaining the required sensitivity and precision to detect radioactive xenon in the atmosphere.

In future work, we will manufacture the phoswich well detector studied above, adapt and optimize the PSA algorithms, evaluate the detector's performance, and compare it in field trials with the existing ARSA detector.

#### REFERENCES

- [1] P. L. Reeder, T. W. Bowyer, and R. W. Perkins, "Beta-gamma counting system for Xe fission products," *J. Radioanal. Nucl. Chem.*, vol. 235, no. 1-2, pp. 89-94, 1998.
- [2] J. H. Ely, C. E. Aalseth, and J. I. McIntyre, "Novel beta-gamma coincidence measurements using phoswich detectors," *J. Radioanal. Nucl. Chem.*, vol. 263, no. 1, pp. 245-250, 2005.
- [3] W. Hennig, Y. X. Chu, H. Tan, A. Fallu-Labruyere, W. K. Warburton, and R. Grzywacz, "The DGF Pixie-4 spectrometer-compact digital readout electronics for HPGe clover detectors," *Nucl. Instrum. Methods Phys. Res. B*, submitted for publication.
- [4] C. Moisan, F. Cayouet, and G. McDonald. DETECT2000: The object oriented C++ language version of Detect: A program for modeling optical properties of scintillators. [Online]. Available: [www.gel.ulaval.ca/detect](http://www.gel.ulaval.ca/detect)